

Measurement of nondegenerate nonlinearities using a two-color Z scan

M. Sheik-Bahae, J. Wang, R. DeSalvo, D. J. Hagan, and E. W. Van Stryland

Center for Research in Electro-Optics and Lasers, University of Central Florida, Orlando, Florida 32816

Received October 9, 1991

A simple dual-wavelength (two-color) Z-scan geometry is demonstrated for measuring nonlinearities at frequency ω_p owing to the presence of light at ω_e . This technique gives the nondegenerate two-photon absorption (2PA) coefficient $\beta(\omega_p; \omega_e)$ and the nondegenerate nonlinear refractive index $n_2(\omega_p; \omega_e)$, i.e., cross-phase modulation. We demonstrate this technique on CS₂ for n_2 and on ZnSe where 2PA and n_2 are present simultaneously.

The newly developed Z-scan technique has been used as an accurate and sensitive tool for determining nonlinear refraction and absorption in a single-beam single-wavelength geometry.¹ Here we introduce a dual-wavelength (two-color) extension of this technique for measuring changes of refraction Δn and absorption $\Delta\alpha$ induced by a strong excitation beam at frequency ω_e on a weak probe beam at a different frequency ω_p ; i.e., $\Delta n(\omega_p; \omega_e)$ and $\Delta\alpha(\omega_p; \omega_e)$, respectively.^{2,3} In the lowest-order nonlinearity such quantities are defined through the third-order susceptibility.

Measurements of these nondegenerate nonlinearities potentially allow determination of material parameters not available from their degenerate counterparts. For example, it has been shown⁴ that the frequency difference ($\omega_p - \omega_e$) can be exploited to obtain information about the dynamics of the nonlinear response with a time resolution much less than the laser pulse width. With ultrashort pulses we can use a time delay between excitation and probing pulses to further give a detailed time-resolved picture of the nonlinear interaction. A recent theory based on the nonlinear Kramers-Kronig transformation predicts dispersion relations between degenerate and nondegenerate nonresonant bound-electronic contributions of Δn and $\Delta\alpha$.⁵ Experiments performed with the single-beam Z scan strongly support the dispersion relations for the degenerate case. The two-color Z scan enables us to investigate the nondegenerate theory experimentally.⁶ From a practical point of view, investigating nondegenerate optical nonlinearities is of interest in the area of dual-wavelength all-optical switching applications in which cross-phase modulation plays an essential role.

The two-color Z-scan experimental arrangement used in these experiments is shown in Fig. 1. Picosecond pulses from a mode-locked Nd:YAG laser ($\lambda = 1.06 \mu\text{m}$) are used as the excitation beam. The copropagating probe is generated by inserting a 3-mm-thick, thin KD*P crystal with a $\approx 1\%$ conversion efficiency in the beam path. The two beams

are then focused with an achromatic lens of focal length $f \approx 15 \text{ cm}$. The transmitted beam is split and sent to two detectors in the far field that each monitor only one wavelength ($\lambda = 0.532$ or $1.06 \mu\text{m}$) as the sample is scanned along the Z direction (propagation path) near the focal plane. Analogous to the usual single-wavelength Z scan, with a fully open aperture (100% transmittance), the measurement is only sensitive to the induced changes in absorption, while a partially closed aperture Z scan displays the induced refractive changes as well. In this geometry, perpendicular polarization results from the type I phase-matched second-harmonic generation. Parallel polarization is obtained by inserting a calcite polarizer before the focusing lens.

In the case of the two-color Z scan, the field consists of a strong excitation beam at frequency ω_e and a weak probe at ω_p . Thus in the weak-probe approximation and for thin samples in the external self-action geometry^{1,4} the propagation of the probe beam within the sample can be fully determined using the following equations:

$$\frac{dI_e}{dz'} = -\alpha_e I_e - \beta_{11}(\omega_e; \omega_e) I_e^2, \quad (1a)$$

$$\frac{dI_p}{dz'} = -2\beta_{12}(\omega_p; \omega_e) I_e I_p, \quad (1b)$$

$$\frac{d\Delta\phi_p}{dz'} = \frac{\omega_p}{c} 2\gamma_{12}(\omega_p; \omega_e) I_e, \quad (1c)$$

where $I_{e,p}$ are the irradiances, which are functions of the depth into the sample z' , the radial coordinate r , the time t , and the sample position Z . The nonlinear phase variation of the probe is given by $\Delta\phi_p$, which is also a function of Z , z' , r , and t . The linear absorption coefficient at the excitation wavelength is α_e , $\beta_{21}(\omega_p; \omega_e)$ and $\beta_{11}(\omega_e; \omega_e)$ denote the nondegenerate and degenerate 2PA coefficients, respectively, and γ_{12} represents the nonlinear refractive coefficient, which can also be given in terms of n_2 (esu).¹ The subscripts 1 and 2 denote the state of polarization of the excitation and probe beams, re-

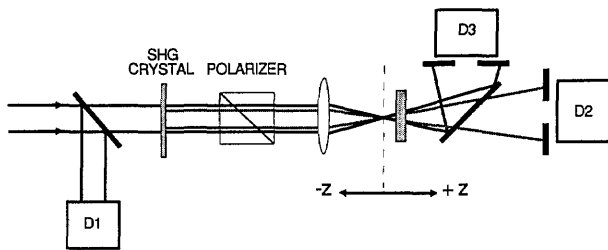


Fig. 1. Two-color Z-scan experimental configuration. The measured signal is the ratio $D2/D1$ as the sample is scanned along the propagation (Z) axis.

spectively, and may correspond to the transverse directions x or y . For example, with the probe and excitation beams perpendicularly polarized, we have $1 = x$ and $2 = y$. Equation (1a) gives the pump depletion caused by 2PA, while Eqs. (1b) and (1c) describe the cross amplitude and the phase modulation of the probe caused by the excitation beam. Note the factor of 2 in front of γ_{12} and β_{12} in Eqs. (1b) and (1c). This factor arises from the interference between excitation and probe fields,^{7,8} and its validity depends on the condition that the response time of the medium τ must be shorter than the beat period; i.e., $\tau|\omega_p - \omega_e| \ll 1$.⁹ This is true for degenerate ($\omega_p = \omega_e$) nonlinearities or nonresonant bound-electronic nonlinearities. For molecular reorientational nonlinearities, such as those in CS_2 ($\tau \approx 2$ ps), this factor of 2 should not be included in the analysis of the nondegenerate case for which $\omega_p - \omega_e = \omega_e$.

The probe is assumed to be sufficiently weak not to induce any self- or cross-modulation effects. The linear absorption, refraction, and surface reflections of the probe beam are immaterial if we normalize the probe transmittance to unity in the absence of any nonlinearity. Equations (1a), (1b), and (1c) can be solved for a sample of length L to give the probe field, which is proportional to $\sqrt{I_p} \exp[-i\Delta\phi(z, r, t, z' = L)]$, at the exit surface of the sample. The far-field electric-field distribution is then calculated from linear-diffraction theory.⁴

The measured quantity in a Z-scan experiment is the normalized transmitted power through the far-field aperture that has a radius r_a with a linear transmittance S as given by $1 - \exp(-2r_a^2/w_a^2)$, where w_a is the beam waist of the probe at the aperture when $I_e = 0$. If we assume pulsed radiation, the measured quantity is the transmitted pulse energy. A full analytical expression can be obtained for the Z-scan transmittance by accounting for the differences in beam sizes, pulse widths, and focal lengths (chromatic aberration).²

We first consider liquid CS_2 where only nonlinear refraction is present [i.e., all β 's = 0 in Eqs. (1)]. The measured two-color Z scans for this material at an excitation irradiance of 2.9 GW/cm^2 are shown in Fig. 2 for cases of parallel and perpendicular polarization. The asymmetry in the two-color Z scan (unequal peak and valley magnitudes) results from the small chromatic aberration ($\Delta f/f \approx 1\%$) of the focusing lens and has been accounted for in the beam propagation analysis. This aberration causes the beam with the shorter wavelength (in this case the

probe) to experience a shorter effective focal length, which leads to unequal peak and valley amplitudes. The peak and valley configuration shows that self-focusing ($\Delta n > 0$) results for parallel polarization and that self-defocusing ($\Delta n < 0$) results for crossed polarizations. Here the excitation beam aligns the cigar-shaped molecules along its polarization (for example, x), which increases the refractive index for light that shares its polarization and reduces the index equally along the other two directions (y and z) for crossed polarization.

Nonlinear refraction in CS_2 arises primarily from the molecular orientation effect (γ_{12}^m) with a ≈ 2 -ps decay time, with small additional contributions from intermolecular, intramolecular, and electronic effects.¹⁰ Here we assume that these latter small contributions, which we denote by γ_{12}^e , are of an electronic type; i.e., they are instantaneous ($|\omega_p - \omega_e|\tau \ll 1$) and isotropic. A simple molecular orientational model predicts that $\gamma_{xx}^m = -2\gamma_{xy}^m$,⁷ while symmetry properties for an isotropic electronic nonlinearity dictate that $\gamma_{xx}^e = 3\gamma_{xy}^e$.⁶ Therefore in a two-color Z-scan measurement we can determine each contribution by equating the total index change as the sum of the electronic and the orientational effects $2\gamma_{xx} = \gamma_{xx}^m + 2\gamma_{xx}^e$, $2\gamma_{xy} = -(\gamma_{xx}^m)/2 + (2\gamma_{xx}^e)/3$, respectively. The solid curves in Fig. 3 are the best-fitted results for CS_2 by using $\gamma_{xy} = -0.67 \times 10^{-14} \text{ cm}^2/\text{W}$ and $\gamma_{xx} = 2.13 \times 10^{-14} \text{ cm}^2/\text{W}$, which gives $\gamma_{xx}^m = 3.3 \times 10^{-14} \text{ cm}^2/\text{W}$ and $\gamma_{xx}^e = 0.47 \times 10^{-14} \text{ cm}^2/\text{W}$. These values indicate that the electronic effect contributes $\approx 15\%$ to the total nonlinear refraction.

Although detailed calculations were performed to fit the above results, such a procedure is not always necessary for estimating γ_{12} . As was the case for the degenerate Z scan, for a given aperture transmittance S and input irradiance, it suffices to know

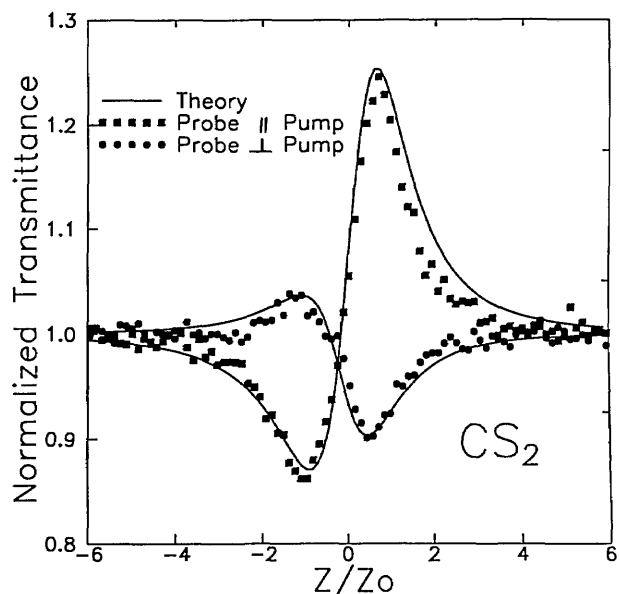


Fig. 2. Measured two-color Z scans ($\lambda = 1.06$ and $0.532 \mu\text{m}$) for liquid CS_2 for parallel (squares) and perpendicular (circles) polarization. The solid curves represent theoretical calculations.

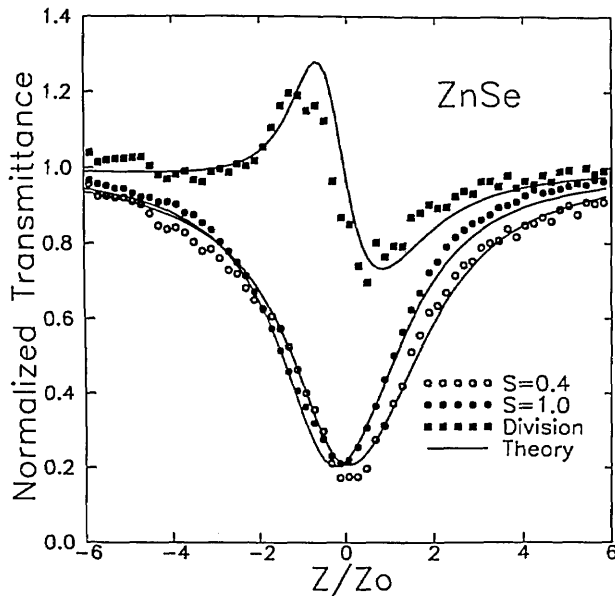


Fig. 3. Normalized transmittance as a function of sample position Z for ZnSe. The solid circles represent the open-aperture Z scan, the open circles represent the closed-aperture Z scan, and the solid squares represent the division of closed by open data values. The lines are from the best-fitted calculations.

only the normalized peak-to-valley transmittance change ΔT_{p-v} , which is defined as the difference between the peak normalized transmittance and the minimum (valley) normalized transmittance. This value is used to extract the peak on-axis phase distortion of the probe ($\Delta\Phi_{12}$) at the exit surface of the sample as derived from Eq. (1c). A useful feature of the Z-scan technique is that for a purely refractive nonlinearity there exists a nearly linear relationship between ΔT_{p-v} and $\Delta\Phi_{12}$ as in the degenerate case,¹

$$\Delta T_{p-v} = p\langle\Delta\Phi_{12}\rangle, \quad (2)$$

where $\Delta\Phi_{12} = \omega_p \gamma_{12} I_{e0}(1 - e^{-\alpha_e L})/c\alpha_e$, with I_{e0} being the peak on-axis irradiance at the beam waist. Numerical analysis indicates that for very small apertures ($S = 0$) and small chromatic aberration, $p \approx 0.42$ for the two-color case, as compared with $p \approx 0.406$ for the degenerate case.¹ Chromatic aberration that results in foci separated by one Rayleigh range can actually increase the sensitivity by up to $\approx 20\%$. The dependence of the p coefficient on the aperture transmittance S is numerically evaluated to approximately follow a $(1 - S)^{0.35}$ dependence. Attention should also be given to the time-averaging factor for the pulsed case, where here $\langle\Delta\Phi_{12}\rangle = \Delta\Phi_{12}/\sqrt{1.5}$ as opposed to $\langle\Delta\Phi_{11}\rangle = \Delta\Phi_{11}/\sqrt{2}$ for the single-frequency Z scan.¹

We next consider ZnSe that has a band-gap energy of $E_g \approx 2.6$ eV for which the degenerate 2PA coefficients are $\beta(1.06 \mu\text{m}) = 0$ and $\beta(0.53 \mu\text{m}) \approx 5.8$ cm/GW.¹ Nondegenerate 2PA with strong 1.06- μm excitation that is probed at 0.53 μm is allowed; i.e., $\beta(0.53 \mu\text{m}; 1.06 \mu\text{m}) \neq 0$. Figure 3 shows the two-color Z scan of a 2.7-mm-thick polycrystalline ZnSe sample. These data are obtained by using orthogonal polarization of the

pump and the probe. From the open aperture ($S = 1$), the data β_{12} can be unambiguously determined by using Eqs. (1). The closed-aperture ($S = 0.4$) Z scan, similar to the degenerate measurements, depends on γ_{12} as well as on β_{12} .¹ The effect of this cross-phase modulation can be made more visible by dividing the closed-aperture data by the open-aperture data as was done for the single-wavelength Z scan.¹ The result of this division, shown in Fig. 3, shows a negative (defocusing) effect.¹ The solid curves in Fig. 3 are the results calculated by using Eqs. (1) with $\beta_{12} = 8.8$ cm/GW and $\gamma_{12} = 2.7 \times 10^{-14}$ cm²/W at a peak pump irradiance of $I_0 \approx 1.0$ GW/cm². The irradiances used are low enough that the negative nonlinear refraction from the 2PA (1.06 μm + 0.53 μm) generated carriers is negligible. Thus this nonlinear refraction is the third-order nondegenerate bound-electronic Kerr effect.⁵

In summary we have demonstrated an extension of the Z-scan technique to measure nonlinearities at one wavelength caused by a second. This two-color Z scan retains the sensitivity and many of the simple features of the degenerate Z scan and yields the sign and the magnitude of nonlinear refraction even in the presence of nonlinear absorption, where it also yields the nonlinear absorption coefficient.

We gratefully acknowledge the Defense Advanced Research Projects Agency/Center for Night Vision and Electro Optics, the U.S. Army Research Office, the U.S. Army Vulnerability Assessment Laboratory, and the Florida High Technology and Industry Council.

References

1. M. Sheik-Bahae, A. A. Said, T. H. Wei, D. J. Hagan, and E. W. Van Stryland, *IEEE J. Quantum Electron.* **26**, 760 (1990).
2. M. Sheik-Bahae, J. R. De Salvo, J. Wang, D. J. Hagan, and E. W. Van Stryland, in *Conference on Lasers and Electro-Optics*, Vol. 15 of OSA 1991 Technical Digest Series (Optical Society of America, Washington, D.C., 1991), paper CTuW16.
3. H. Ma, A. S. L. Gomes, and C. B. de Araujo, *Appl. Phys. Lett.* **59**, 2666 (1991).
4. R. Adair, L. L. Chase, and S. A. Payne, *J. Opt. Soc. Am. B* **4**, 875 (1987).
5. M. Sheik-Bahae, D. C. Hutchings, D. J. Hagan, and E. W. Van Stryland, *IEEE J. Quantum Electron.* **27**, 1296 (1991).
6. M. Sheik-Bahae, D. C. Hutchings, D. J. Hagan, and E. W. Van Stryland, in *Quantum Electronics Laser Science*, Vol. 11 of 1991 OSA Technical Digest Series (Optical Society of America, Washington, D.C., 1991), paper QTuI16.
7. E. W. Van Stryland, A. L. Smirl, T. F. Boggess, M. J. Soileau, B. S. Wherrett, and F. A. Hopf, *Chem. Phys.* **23**, 368 (1982).
8. P. N. Butcher and D. Cotter, *Elements of Nonlinear Optics* (Cambridge U. Press, New York, 1990).
9. N. Bloembergen and P. Lallemand, *Phys. Rev. Lett.* **16**, 81 (1966).
10. D. McMorrow, W. T. Lotshaw, and G. A. Kenny-Wallace, *IEEE J. Quantum Electron.* **24**, 443 (1988).